Journal of Nuclear Materials 176 & 177 (1990) 1076–1082
North-Holland

Edge plasma investigation on the reversed field pinch ETA BETA II

V. Antoni, M. Bagatin, A. Buffa, G. Della Mea *,§, D. Desideri, F. Freyre Jr. +, P. Mazzoldi * and F. Romanato *

Istituto Gas Ionizzati del CNR, Associazione Euratom–ENEA–CNR, Padova, Italy

The boundary region of the ETA BETA II RFP experiment has been investigated by movable instrumented limiters equipped with Langmuir probes, heat flux probes, and surface collectors.

Edge plasma temperature and density are of the order of 10 eV and $0.5–1\times10^{19}$ m^{-3}. The heat deposition on the movable limiter is asymmetric between the electron and the ion drift side, and a power flux of the order of 300 MW/m^2 is measured on the electron drift side. This high value has been explained by the presence of current carrying electrons coming from the hotter region of the plasma, through a stochastic region extending into the plasma.

Surface collectors have been inserted in the plasma and analyzed by RBS and ERD techniques. The implanted impurities are mainly oxygen and metallic elements of the liner, both showing a quite linear build up as a function of the exposure time, whereas the amount of trapped deuterium tends to a stationary value after a few discharges. The deuterium flux incident on the wall has been inferred, the impurity yield estimated, and the generation mechanisms discussed.

The deposition radial profiles give information on the screening capability of the boundary region. The estimate of the transmitted impurity flux appears in agreement with what is expected in terms of the known impurity content in the discharge. The stochastic behaviour of the magnetic field in a wide portion of the plasma near the wall is suggested to improve an uniform thermal load, and a more effective screening of heavy impurities.

1. Introduction

The magnetic field of a reversed field pinch (RFP) configuration is produced by mainly internal currents. The safety factor $q = rB_z/RB_\theta$ is lower than 1 and of the order of $-1/10$ near the wall where the toroidal magnetic field is small and changes sign [1]. A plasma confined by this configuration is characterized by a substantial level of magnetic fluctuation ($b/B \approx 1\%$ at plasma currents of the order of some 100 kA), which exhibits mainly $m = 1$ and $m = 0$ poloidal periodicity, both spread on a wide toroidal periodicity spectrum [2]. These fluctuations are interpreted in terms of ideal and resistive MHD instabilities, whose growth and non-linear interaction result in a large plasma volume where the magnetic field lines wind ergodically. The anomalous energy transport measured in present experiments can be related to this fully stochastic region which deteriorates the electron confinement [3]. The enhanced transport results in a large thermal load on the first wall of RFP experiments and in asymmetric energy deposition in the electron drift direction [3,4] due to current carrying electrons coming from the hotter region of the plasma through the stochastic region and hitting the wall without undergoing collisions.

The investigation of Plasma Surface Interaction processes in RFP's has been devoted to the study of different graphite limiter configurations and to the effect of field errors and plasma position control [5–11]. The results contributed to the design of the first wall of the next generation of such devices, namely RFX [12], under construction at Padova, and ZT-H [13], under construction at Los Alamos.

On ETA BETA II, the experiment at present operating at Padova, Langmuir probes, heat flux probes, and surface collectors have been inserted in the outer region of the plasma. After exposure the surface collectors

* Unità INFM, Dipartimento di Fisica, Università di Padova, Italy
§ Dipartimento di Ingegneria dei Materiali, Università di Trento, Italy.
+ Permanent address: Departemento de Fisica PUC/RJ, Brazil.

0022-3115/90/$03.50

have been transferred in air to a surface analysis facility. The status of the surfaces has been surveyed by scanning electron microscopy (SEM) and then the samples have been analyzed by elastic recoil detection (ERD) and Rutherford backscattering spectroscopy (RBS) techniques [14]. From the dose of implanted particles the impurity and deuterium fluxes have been inferred. The screening capability of the outer region of the plasma has been investigated by comparing the impurity flux transmission with the known content of the plasma bulk.

2. Experiment

In fig. 1 the plasma current I_ϕ and electron density n_e waveforms of the ETA BETA II, the toroidal device with major radius $R = 0.65$ m and minor radius $a = 0.125$ m [15] at present operating at Padova, are reported. At $I_\phi \sim 150$ kA, the corresponding electron temperature on axis and average electron density are $T_e \sim 150$ eV and $n_e \sim 5 \times 10^{19}$ m^{-3} respectively. The duration of the current flat top phase is $\tau \sim 1.5$ ms.

The vacuum vessel is an AISI 316 stainless steel bellows whose minor radius of the convolution is 12.5 cm inside and 13.5 cm outside, with plane sections of minor radius 13.5 cm in correspondance to the port-holes.

In fig. 2 the equipment used for the insertion of the probes is shown. It consists of a rack and pinion linear translator with a 360° rotational capability. The probes are mounted on the top of the moving rod. In particular the sample holder has been inserted up to 11.5 cm from the geometric minor axis of the device, i.e. 1 cm beyond the bellows inner convolution of the vacuum chamber. A schematic view of the surface collector holder is shown in fig. 3. It is instrumented with thermocouples to detect the incident power flux. The tiles protecting the Langmuir probes and the sample holder are made of

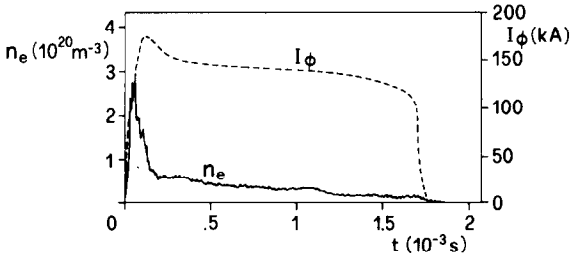

Fig. 1. Plasma current and density waveforms.

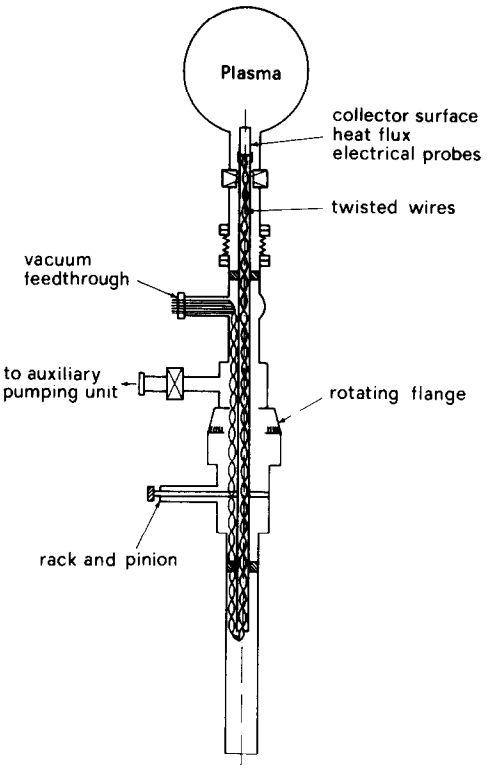

Fig. 2. Scheme of the experimental apparatus.

Ringsdorff EK 98 polycrystalline graphite, the surface collectors of Carbon Lorraine vitreous graphite V 25. The sample holder has been inserted in the outer region so as to keep the surface collectors normal to the magnetic field lines.

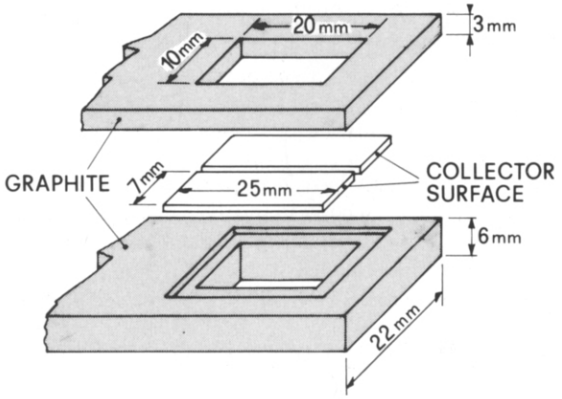

Fig. 3. Scheme of the sample holder equipment.

Since the experiment does not provide a plasma position control by a vertical field, the plasma column shifts outwards. The displacement (typically < 1 cm [16]), combined with the bellows convolution, creates a cooler layer in the outer region where the magnetic field lines intercept the liner, and whose radial extension can be estimated of the order of 1 cm. Since the probes are inserted in a pipe located in a plane section of the liner, the wall has been fixed at a radial position $r = 13.5$ cm, where the origin of the slab coordinates, used in this context, has been taken.

The protection tiles and the sample holder, inserted in the plasma, act as poloidal limiters, and create locally, a Scrape Off Layer (SOL), with a poloidal connection length of the order of half the minor circumference. The probe insertion up to 1–2 cm from the wall, does not change significantly the plasma performance. The power flux intercepted by these limiters shows a strong directionality with the magnetic field [4,11], and it can reach, on the electron drift side, maximum values of the order of 300 MW m^{-2} just inside the inner convolution of the bellows [11], and almost an order of magnitude lower on the opposite side. The spatial behaviour shows an exponential decay towards the wall with an e-folding length of the order of 0.5–1 cm depending on the insertion depth of the limiter [11].

For similar discharges where Langmuir probes have been inserted, typical values of electron temperature and density at the edge are $T_e \sim 10$ eV and $n_e \sim (0.5\text{–}1) \times 10^{19}$ m^{-3} with e-folding length $\lambda_T \sim 2\text{–}3$ cm and $\lambda_n \sim 1\text{–}2$ cm. The floating potential at a distance of 1 cm from the wall is ≈ -30 V, so that the ion incident energy is expected to be ≈ 40 eV for deuterium and larger (≈ 100 eV) for multiple charged impurity ions. From the ion saturation current collected by Langmuir probes, the charged particle parallel flux is estimated to be of the order of 3×10^{23} m^{-2} s^{-1} (within a factor 2 of uncertainty on the probe collection surface), with an e-folding length $\lambda_\Gamma \sim 0.5\text{–}1$ cm.

3. Surface collector results

Surface collectors have been exposed to the plasma for 1, 5, and 15 discharges, and then have been transferred in air to be analyzed by nuclear techniques [14]. The deuterium and impurity concentration in the surface collectors have been investigated by elastic recoil detection (ERD) and by Rutherford backscattering spectrometry (RBS) using 2 MeV $^4He^+$ beams with a current density of 4mA/cm^2 obtained from a 2.5 MV Van de Graaf accelerator [17]. The size of the beam analyser spot was 1×0.5 mm^2 with a lateral resolution of 0.1 mm.

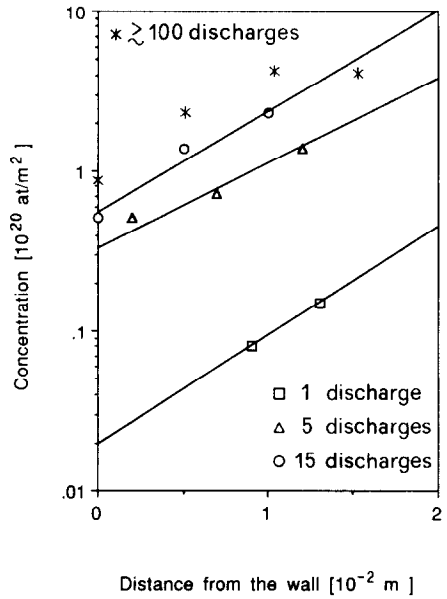

Fig. 4. Deuterium dose measured in a vitreous graphite collector surface exposed to 1, 5 and 15 discharges. For comparison the dose measured on protection tiles after ~100 discharges is also reported.

Before that, the surface status of the samples was surveyed by scanning electron microscopy (SEM). As a general feature, the surface of the targets appears more eroded on the electron drift side. The excessive roughness of the graphite surfaces on the electron drift side prevented a quantitative analysis by RBS and ERD, so that it has been restricted to the ion drift side [14].

Fig. 4 shows the deuterium dose versus X, the distance from the wall, in the ion drift side of the surface collectors exposed to different numbers of discharges. The retained deuterium concentration shows an exponential increase with the distance from the wall with an e-folding length $\lambda_D \sim 0.75$ cm. For comparison on the same figure is also reported the dose measured after about 100 shots on the polycrystalline graphite of the tiles protecting the Langmuir probes.

It has been found [14] that deuterium in vitreous graphite tends to saturate after 15 discharges, at a value of 3×10^{20} at/m^2. Assuming an uniform implantation, this dose corresponds to a saturation depth of about 7 nm with a 0.4 D atom per C atom fractional concentration [18]. Assuming this penetration depth as the maximum projected range, a TRIM code simulation limits the energy of incident deuterium to less than 100 eV.

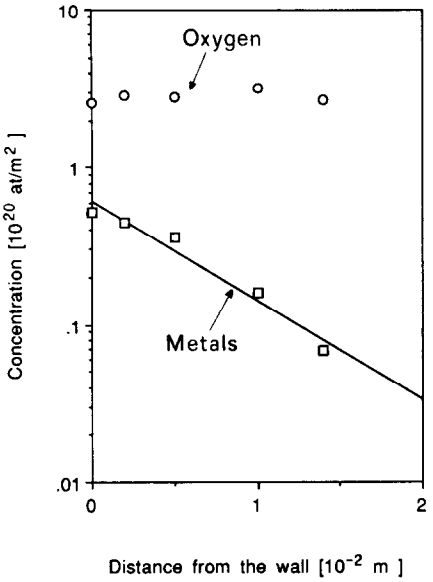

Fig. 5. Dose of oxygen and metals measured in a vitreous graphite collector surface exposed to 15 discharges.

The implanted dose of deuterium, corrected by the backscattering coefficient (≈ 0.5 for 40 eV deuterium ions incident on graphite) should be proportional to the incident parallel deuterium flux. However the flux per discharge, obtained from the implanted dose, results an order of magnitude lower than expected, also taking into account the backscattering coefficient. In fact the global deuterium flux of about 3×10^{23} m^{-2} s^{-1}, as estimated by Langmuir probe measurements, corresponds to a deuterium fluence per discharge of the order of 3×10^{20} m^{-2}. The discrepancy has been accounted by the fact that the low energy incident ions ($\sim$ 40 eV) saturates in one shot the first monolayers of the graphite sample.

Metals and oxygen are the main impurities detected by RBS analysis, and both show an almost linear build-up with the number of discharges [14]. Since graphite has a lower mass, backscattering and desorption can be neglected, and therefore a sticking coefficient of 1 has been assumed.

Fig. 5 shows the deposition of oxygen and metal impurities on the same vitreous graphite samples, of fig. 4, showing different spatial behaviours. The metal concentration decays towards the plasma with an e-folding length $\sim$ 1 cm. It has been found [14] that the metal concentration has the same chemical composition of the vacuum vessel material AISI 316 stainless steel, and the metal fluence per discharge, is $\sim 0.4 \times 10^{19}$ m^{-2}.

On the other hand oxygen analysis is controversial due to possible chemical modifications during transportation in air of the samples [19]. However, the measured oxygen dose has not stoichiometric relationship with the metal concentration and its spatial distribution in the sample does not show any correlation with metal distribution. In addition, its build up shows an approximately linear increase with the exposure time from an initial background value of about 1.3×10^{20} m^{-2} to a final value of $\sim 3 \times 10^{20}$ m^{-2}. Assuming that the implanted oxygen is proportional to the ion incident flux [20], the inferred fluence is of the order of 10^{19} m^{-2} per discharge.

4. Discussion

In the present case the decay length $\lambda_D \sim 0.75$ cm, derived from the deuterium retained dose, has been assumed to be representative of the deuterium flux decay length λ_Γ. With electron temperature and heat flux decay lengths in the range mentioned above, the density decay length can be estimated to be $\lambda_n \approx 1$ cm. It is worth noting that it gives, assuming a simple SOL, a particle diffusion coefficient at the edge, $D = \lambda_n^2 C_s / L$, ≈ 10 m^2 s^{-1}, where C_s is the ion sound velocity, and L is the connection length.

On the other hand the perpendicular ion flux diffusing from the plasma to the wall $\Gamma_\perp$, can be estimated by dividing the parallel flux, measured by Langmuir probes, by the geometrical intensification factor L/λ_{ls}, where λ_{ls} is the ion saturation current radial decay length on the shadow of the protection tile, and it results in $\Gamma_\perp \approx 4 \times 10^{21}$ m^{-2} s^{-1}.

The effective fraction of impurities $\alpha = n^{imp}/n_e$ penetrating into the plasma can be estimated through a simple equation governing the impurity build up in the plasma [21]:

$$\frac{\partial \alpha}{\partial t} = (\eta Y - \alpha)\frac{1}{\tau_p},$$

whose solution is $\alpha(t) = \eta Y(1 - e^{-t/\tau_p})$, where η represents the SOL transmission factor, Y is the impurity equivalent yield for incident deuterium flux, α/τ_p represents the impurity exhaust, and the same particle confinement time τ_p is assumed for deuterium and impurities. Since the pulse length $\tau \gg \tau_p$, a value of α comparable to the final saturation value ηY is achieved very early during the discharge [21]. From spectroscopic measurements the typical impurity concentration on ETA BETA II are known to be $\alpha \sim 1$–3% for oxygen and $\alpha \sim 0.1\%$ for metals [22].

The measured concentrations of deuterium and impurities on the deposition probes can be discussed in terms of a simple model in which the implanted ions may be either neutrals coming from the wall and ionized in the SOL, or ions diffusing from the plasma. Separating the respective contributions, this model can also give some insight into the deuterium recycling and impurity screening in the outer region.

The impurity radial fluxes Γ_w^{imp} (neutrals released by the wall) and Γ_p^{imp} (ions diffused by the plasma) are functions of the radial distance from the wall X. In particular the neutral flux released at the wall $\Gamma_w(0)$ is given by the product of the deuterium outflux Γ_D times an equivalent impurity yield Y as $\Gamma_w(0) = Y\Gamma_D$.

The attenuation of the flux of neutrals released with velocity v_0 and ionized by electron impact (charge-exchange is neglected) is given by:

$$\Gamma_w^{imp}(x) = \Gamma_w^{imp}(0)\exp\left(-\int_0^x \frac{n_e(x')S(x')}{v_0}\,dx'\right),$$

where $S(x)$ is the collisional ionization rate coefficient that in the present discussion has been taken by ref. [23].

Assuming a thickness h of the equivalent SOL in the outer region, so that the neutrals ionized at $x > h$ enter into the plasma, the ratio $\eta = \Gamma_w(h)/\Gamma_w(0)$ defines the transmission factor of the SOL. If the average electron density and temperature are assumed constant in the SOL, thus the flux decay is simplified as:

$$\Gamma_w^{imp}(x) = \Gamma_w^{imp}(0)\exp(-x/\lambda_i),$$

where $\lambda_i = v_0/n_e(0)S(0)$ is the ionization mean free path of the impurity.The contribution to the impurity concentration found on surface collectors is given by the spatial derivative of the neutral flux multiplied by the connection length $L = \pi a$ and the pulse length τ. In particular the concentration at the wall is defined as $C(0) = \Gamma_w(0)L\tau/\lambda_i$.

The experimental concentration of metals, reported in fig. 5, shows that these impurities are almost fully screened in the first centimetre from the wall, thus indicating that a predominant role of the Γ_w^{imp} contribution should be expected. In this case by evaluating the attenuation in the first two centimetres with the measured profiles of electron density and temperature in the outer region (i.e. $T_e = 10$ eV constant and $n_e(0) = 2.5 \times 10^{18}$ m^{-3}, increasing towards the plasma with $\lambda_n = 1$ cm) and using v_0 corresponding to energies of 2 eV, typical of sputtered atoms [24], the neutral flux and metal concentration, obtained for one discharge, are shown in fig. 6. The concentration profile exhibits a substantial agreement with the experimental values ob-

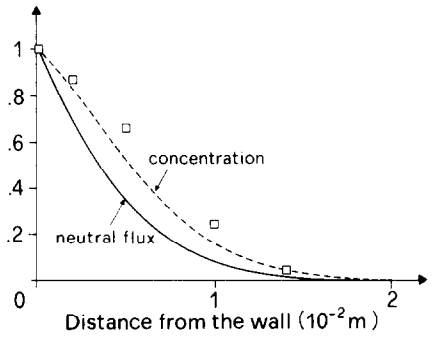

Fig. 6. Metal impurity neutral flux and concentration (dashed line), both normalized to the value at the wall, as a function of the distance from the wall. The dots refer to the experimental concentration for one discharge. The concentration and the flux at the wall ($X = 0$) are respectively $C(0) = 3.6\times10^{18}$ m^{-2} and $\Gamma_w(0) = 3.5\times10^{19}$ m^{-2} s^{-1}.

tained by normalizing to one the concentration for 15 discharges of fig. 5. In particular, the effective yield for metal impurity generation $Y = \Gamma_w^{imp}(0)/\Gamma_D$ is about 10^{-2}. The experimental metal concentration in the bulk, of the order of 10^{-3}, can be therefore justified by a transmission factor $\eta \sim 10\%$, which in turn is consistent with an equivalent SOL thickness $h \sim 1$ cm.

The experimental deposition profile for oxygen is, on the other hand, rather flat, indicating a non-negligible role of the contribution from the plasma. Nevertheless the plasma contribution in first approximation has been neglected, and the attenuation calculated assuming, as for metals, v_0 corresponding to 2 eV, typical of ion induced desorbed oxygen. In this case $\lambda_i \gg h$ and η almost equal to 1 have been found, resulting in unacceptably high values of oxygen content in the plasma and producing, in addition, deposition profiles with rising slope towards the plasma. Reducing the initial velocity v_0 to 0.5 eV, i.e. typical of thermally desorbed oxygen neutrals or molecules, the curves illustrated in fig. 7 are found. From the computed profiles, values of $Y \cong 10\%$ and $\eta = 50\%$, evaluated at $X = 1$ cm, are found, corresponding to $\alpha \sim 5\%$, which is somewhat larger than the experimental content. It is worth noting that this value can be further reduced assuming lower temperature or molecular oxygen.

By applying the same arguments to deuterium deposition, in which case Y must be replaced by a recycling factor, that was estimated from D_α measurements to be ~ 0.9 [15], we find $\lambda_i \gg h$ and η almost equal to 1, meaning that no significant ionization of recycled deuterium is expected in the SOL. The deposited deuterium concentration is consequently determined by

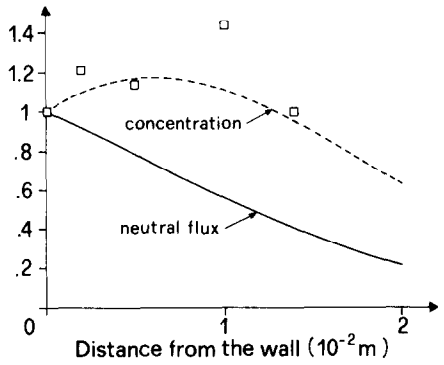

Fig. 7. Oxygen neutral flux and concentration (dashed line), both normalized to the value at the wall, as a function of the distance from the wall. The dots refer to the experimental concentration for one discharge. The concentration and the flux at the wall ($X = 0$) are respectively $C(0) = 8.9 \times 10^{18}$ m^{-2} and $\Gamma_w(0) = 3.8 \times 10^{20}$ m^{-2} s^{-1}.

the ion flux coming from the plasma, according to the experimental profiles shown in fig. 4.

The mechanisms which could be responsible for impurity generation in ETA BETA II are desorption, both thermal and particle induced, for oxygen, and evaporation and sputtering for metals.

The detection on the collector probes of metals in the same elemental composition of the liner alloy suggests that the role played by thermal evaporation of the liner is not dominant. Indeed if thermal effects were important, a much higher relative concentration of chromium, by far the most volatile element of the alloy, should be found. Thus, thermal effects do not seem to be important for metals, according to the fact that the thermal load, even if rather strong, tends to be uniformly distributed by the stochastic behaviour of magnetic field lines in the outer region.

On the other hand, also primary sputtering due to deuterium ions cannot produce metal fluxes at the rate measured by the deposition probes ($Y \sim 10^{-2}$), since the expected energy of the incident ions is of the same order of the sputtering threshold of deuterium on stainless steel (~ 40 eV). Such rates can only be accounted by impinging particles with energies of the order of 100 eV, like, for example, neutrals coming from the bulk plasma, or by secondary sputtering of impurity ions recycled at the edge.

Concerning the oxygen generation, both the energy of desorbed neutrals (≤ 0.5 eV), and their calculated desorption yield ($Y \sim 0.1$) indicate that the main mechanism should be thermal desorption of atoms or molecules.

In conclusion, the most probable candidates, among the impurity production mechanisms, are suggested to be thermal induced desorption for oxygen and sputtering processes for metals.

5. Conclusions

The fluxes of particles coming from the plasma and of neutral impurity released from the wall have been inferred by the deuterium and metal impurity concentration measured on surface collectors exposed to the plasma. The deuterium flux is almost an order of magnitude lower than the value measured by Langmuir probes due to the quick saturation of the first monolayers of the graphite sample.

Metal impurities exhibit a steep decay towards the plasma in agreement with the low global content measured in the bulk plasma. This result proves that the outer region of the plasma is quite effective in screening heavy impurities. The generation mechanism can be mainly accounted by sputtering due to energetic ions or neutrals. Thus the outer region seems to be effective also in spreading quite uniformly the wall loading so to prevent thermal ablation processes. This property of the outer region can be accounted by the stochastic behaviour of magnetic field lines.

On the other hand the oxygen concentration on the surface collectors does not exhibit any spatial structure, suggesting that the measured concentration is the result of the flux coming from the wall and of that coming from the plasma. The resulting transmission factor of the outer region is consistent with the experimental concentration of oxygen in the plasma. The neutral yield is consistent with ion induced thermal desorbtion of monoatomic and molecular oxygen.

Thus the combination of the bellows convolution, plasma column displacement and stochastic region act as an effective SOL, whose depth can be estimated of the order of 1 cm.

The presence of currents driven by electrons flowing along the stochastic magnetic field lines and the relevant contribution due to the ionization of neutral particles released by the wall, indicate that a complex SOL model should be required to describe the properties of the outer region. However, even in the simple SOL approximation used in this context, despite the higher thermal load due to the increased transport, a stochastic region in the outermost plasma seems to be effective in spreading quite uniformly the heat power at the wall and in improving the screening of the heavy impurities realeased by the wall.

References

[1] H.A.B. Bodin and A.A. Newton, Nucl. Fusion 10 (1980) 1255.

[2] V. Antoni, in: Int. School of Plasma Physics, Varenna 1987, Proc. of the Course on Physics of Mirrors, RFP and Compact Tori, Commission of the European Communities EUR 11335. EN, Vol. I, p. 431.

[3] J.C. Ingraham et al., Phys. Fluids B2 (1) (1990) 143.

[4] V. Antoni, M. Bagatin and D. Desideri, in: Proc. Int. Conf. on Plasma Physics, New Delhi, 1989, Vol. I, p. 141.

[5] T.E. Cayton et al., J. Nucl. Mater. 145–147 (1987) 71.

[6] A.A. Newton et al., J. Nucl. Mater. 145–147 (1987) 487.

[7] G.L. Jackson et al., J. Nucl. Mater. 145–147 (1987) 470.

[8] Y. Yagi et al., J. Nucl. Mater. 162–164 (1989) 702.

[9] A. Matsuoka et al., J. Nucl. Mater. 162–164 (1989) 804.

[10] H. Toyama et al., in: Proc. 16th Eur. Conf. on Controlled Fusion and Plasma Physics, Venice, 1989, Vol. II, p. 737.

[11] V. Antoni, M. Bagatin and P. Noonan, Istituto Gas Ionizzati internal report, IGI 89/01.

[12] F. Elio, F. Gnesotto, R.M. Pauletti and P. Sonato, in: Proc. of 14th Symp. on Fusion Engineering (IEEE, New York, 1987) Vol. I, p. 513.

[13] J.N. Downing, K.A. Werley and M.T. Gamble, in: Proc. of the 12th Symp. on Fusion Engineering (IEEE, New York, 1987), Vol. I, p. 503.

[14] V. Antoni et al., Investigation of the ETA BETA II plasma edge by surface analysis of collector probes, submitted to Il Nuovo Cimento.

[15] V. Antoni et al., in: Proc. 12th Int. Conf. on Plasma Physics and Controlled Nuclear Fusion Research, Nice, 1988, Vol. II, p. 661.

[16] V. Antoni, P. Martin and S. Ortolani, Nucl. Fusion 29 (1989) 1759.

[17] P. Mazzoldi and G. Della Mea, Thin Solid Films 77 (1981) 181.

[18] W. Moeller and J. Roth, in: Physics of Plasma-Wall Interactions in Controlled Fusion, Eds. D.E. Post, R. Behrisch (Plenum Press, New York, 1986) NATO ASI Series B: Physics, Vol. 131.

[19] J.P. Coad, J.C.B. Simpson and G.F. Neill, JET internal report, JET - P (89) 08.

[20] E. Vietzke et al., J. Nucl. Mater. 145–147 (1987) 425.

[21] M. Bagatin, S. Costa and S. Ortolani, J. Nucl. Mater. 162–164 (1989) 818.

[22] S. Ortolani, M.E. Puiatti, P. Scarin, G. Tondello, Plasma Phys. and Contr. Fusion 27 (1985) 69.

[23] C. De Michelis and M. Mattioli, Nucl. Fusion 21 (1981) 677.

[24] S.K. Erents et al., Nucl. Fusion 26 (1986) 1591.